Bioorganic & Medicinal Chemistry Letters 25 (2015) 2985–2990

Contents lists available at ScienceDirect

Bioorganic & Medicinal Chemistry Letters

journal homepage: www.elsevier.com/locate/bmcl

Discovery of novel pyrazole-containing benzamides as potent RORγ inverse agonists

Tao Wang [a,*], Daliya Banerjee [b], Tonika Bohnert [a], Jianhua Chao [a], Istvan Enyedy [a], Jason Fontenot [b], Kevin Guertin [a], Howard Jones [a], Edward Y. Lin [a], Douglas Marcotte [a], Tina Talreja [a], Kurt Van Vloten [a]

[a] Chemistry and Molecular Therapeutics, Biogen, 12 Cambridge Center, Cambridge, MA 02142, USA
[b] Immunology Discovery, Biogen, 12 Cambridge Center, Cambridge, MA 02142, USA

ARTICLE INFO

Article history:
Received 29 March 2015
Revised 8 May 2015
Accepted 12 May 2015
Available online 22 May 2015

This Letter is dedicated to Professor Iwao Ojima for the occasion of his 70th birthday

Keywords:
RORγ inverse agonist
IL-17
Inflammation
Autoimmune disease
Th17 cell

ABSTRACT

The nuclear receptor RORγ plays a central role in controlling a pro-inflammatory gene expression program in several lymphocyte lineages including TH17 cells. RORγ-dependent inflammation has been implicated in the pathogenesis of several major autoimmune diseases and thus RORγ is an attractive target for therapeutic intervention in these diseases. Starting from a lead biaryl compound **4a**, replacement of the head phenyl moiety with a substituted aminopyrazole group resulted in a series with improved physical properties. Further SAR exploration led to analogues (e.g., **4j** and **5m**) as potent RORγ inverse agonists.

Recently, the nuclear receptor Retinoic Acid Receptor (RAR)-related orphan receptor C (NR1F3; RORC; RORγ) has emerged as an attractive target for therapeutic intervention in human autoimmune diseases.[1,2] RORγ is expressed in several lymphocyte populations including T cells, γδ T cells, and group 3 innate lymphoid cells and its activity has been demonstrated to be critical for driving a pro-inflammatory gene expression response in these cells.[3–5] These cells produce several pro-inflammatory cytokines, including IL-17a, IL-17f, GM-CSF and IL-22. These cytokines are implicated in autoimmune disease, and their expression is regulated by RORγ activity. Biologics targeting these cytokines, most notably IL-17a and IL-17f, have demonstrated efficacy in human disease.[6] Small molecule inhibitors of RORγ have also demonstrated efficacy in animal models.[7–14] Examples of recently reported RORγ inverse agonists include TMP778 (**1**), GSK805 (**2**) and compound **3**.[15,16] We herein report the discovery of a series of novel pyrazole-containing benzamides as potent RORγ inverse agonists (Fig. 1).

We have recently identified compound **4a** from a biaryl benzamide series as an RORγ inverse agonist (Table 1).[17] It is potent in RORγ biochemical FRET assay (IC_{50}: 29 nM),[18] moderately potent in RORγ GAL4 cellular reporter assay[19] (EC_{50}: 98 nM) and is weakly active in the mouse splenocyte IL-17 assay (895 nM). With a *c*log*P* value greater than 5.0, compound **4a** has poor kinetic aqueous solubility (0.3 μg/mL) and is highly bound to human and rat plasma proteins (0.3% and 0.2% free, respectively). It is reasoned that a replacement of the phenyl head ring with a heteroaryl group would lower the lipophilicity of the molecule and might help improve the physical properties such as solubility. For example, the *c*log*P* of compound **4b** at 4.0 is one log unit lower than its phenyl counterpart **4a**. As shown in Table 1, pyrazole analogue **4b** indeed has an improved aqueous solubility of 32 μg/mL and has single digit free unbound fractions against human/rat plasma proteins. However, there is a significant drop of biochemical and cellular potency for **4b**. We sought to explore more SAR around this newly installed pyrazole ring. Two regioisomers **4c** and **4d** that do not contain the primary amide groups were made. Compound **4c** has a weaker potency as compared to that of **4b**. This result is expected as the carbonyl group from the primary amide of compound **4a** is believed to make an important hydrogen bond interaction with backbone NH of Glu379 of human RORγ protein based on docking analysis (see Fig. 2B in the crystal structure section). Compound **4d**, also devoid of this H-bond interaction, somehow is in the similar potency range to that of **4a**. As 5-membered pyrazole ring is smaller in size as to a 6-membered phenyl ring, analogue **4e** was synthesized and it appears that one extra

* Corresponding author.
E-mail address: taowang2@gmail.com (T. Wang).

http://dx.doi.org/10.1016/j.bmcl.2015.05.028
0960-894X/

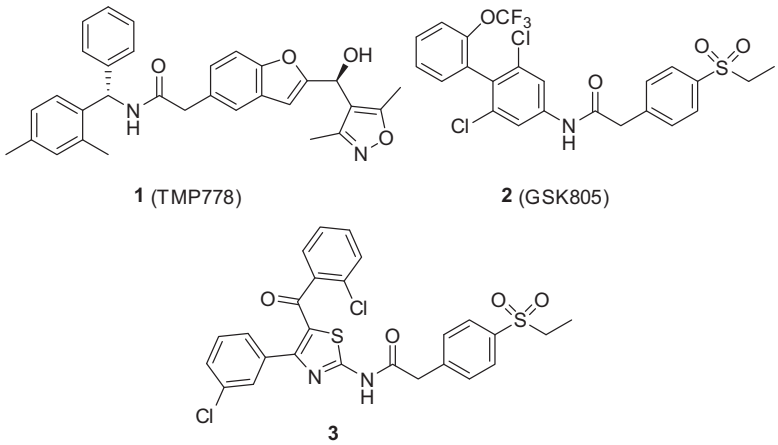

Figure 1. Recent RORγ inverse agonists with in vivo activities.

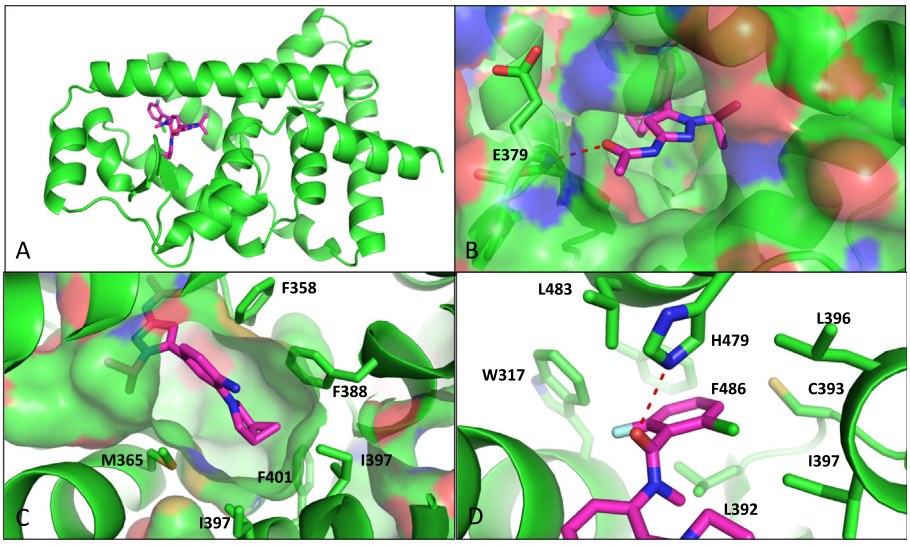

Figure 2. (A) Structure of RORγ bound to **4j**. (B) Backbone interaction between the acetamide carbonyl of **4j** and the backbone amide of E379 at the entrance of the ligand binding site. (C) Central ring orienting azabicyclo[3.1.0] into the hydrophobic subpocket. (D) Tail benzamide sitting in the hydrophobic pocket made by the junction of helix 3, 6, 7 and 11 while the amide carbonyl makes a hydrogen bond with H479.

methylene spacer did not bring the potency back to the level of **4a**. However, acetamide **4f** showed comparable potency in both biochemical and cellular reporter assays. In addition, **4f** exhibited an improved solubility of 27 μg/mL.

With **4f** in hand, we went to investigate the substitutions off the middle phenyl ring (Table 2). A cyclobutylmethoxyl analogue **4g** showed a 5-fold improvement in the RORγ GAL4 reporter assay as compared to **4f** but had weak activity in the mouse splenocyte IL-17 assay (3.1 μM). It is not clear what is causing the larger-than-expected potency shift from Gal4 assay to the mouse splenocyte assay. **4g** has reasonable isoform selectivity over RORα/RORβ based on cellular reporter assays. Closely related oxygen-linked analogues such as **4h** and **4i** both have comparable potency to that of **4f**. The nitrogen-linked substitutions, however, resulted in more potent compounds. Azabicyclo[3.1.0]hexane substituted analogue **4j** has single digit nM potency in the RORγ reporter assay and is 38 nM in the splenocyte IL-17 assay. It has good selectivity over RORα/RORβ and PXR receptor. Physical properties (e.g., solubility) and plasma binding are both improved as to biaryl analogue **4a**. Compound **4j** has an oral exposure of 1045 ng h/mL when dosed in rats at 10 mpk (0–7 h, CMC/Tween) and 2834 ng h/mL when dosed in mouse at 25 mpk (CMC/Tween). The oral exposure in rat is comparable to that of **4a** (3134 ng.hr/mL). Pyrrolidine and piperidine analogues **4k** and **4l** both showed excellent cellular potencies. A pheny analogue **4m** has slightly decreased cellular potency compared to **4j**.

Next, we fixed the middle ring substitution with the azabicyclo[3.1.0]hexane moiety and checked the SAR around the tail benzamide region (Table 3). Regarding R^3 substitution, incorporation of deuterium atoms has attracted a growing interest as it has potential for benefits on profiles (such as reduced metabolism or change of ratio between the metabolites) from the deuterium kinetic isotope effect.[20] In our hands, the profile of **4n** (R^3 equals to CH_3) tracks well with that of **4j** and the 3-fold decrease in the splenocyte activity for **4n** could be within experimental error. For R^4/R^5, Cl/Cl and F/Me substitutions gave analogues **4o** and **4p** with similar RORγ GAL4 activities but with reduced mouse splenocyte potencies. Incorporation of a nitrogen atom to the central ring

Table 1
Replacement of phenyl head ring with a pyrazole

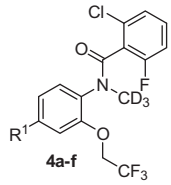

4a-f

Compd ID	R^1	RORγ Fret IC_{50} (nM)	RORγ Gal4 EC_{50} (nM)	Splenocyte IL17 EC_{50} (nM)	Solubility (μg/mL)	PPB fu% Human/rat
4a	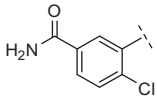	29	98	895	0.3	0.3/0.2
4b	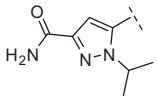	240	570	2000	32	5.9/3.1
4c	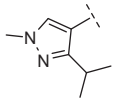	530	1700	–	–	–/–
4d	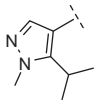	38	160	818	<0.1	0.9/0.6
4e	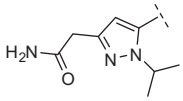	610	1200	–	–	–/–
4f	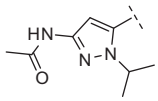	26	160	–	27	–/–

Table 2
SAR at R^2 position

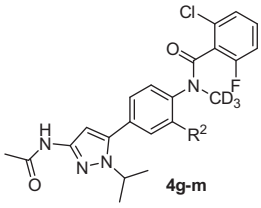

4g-m

Compd ID	R^2	RORγ Fret IC_{50} (nM)	RORγ Gal4 EC_{50} (nM)	Splenocyte IL17 EC_{50} (nM)	RORα/RORβ EC_{50} (μM)	PXR act. EC_{50} (μM)	Solubility (μg/mL)	PPB fu% Human/rat
4g		18	30	3110	1.2/0.9	>10	–	–/–
4h		76	180	–	–/–	–	–	0.3/0.2
4i	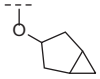	54	130	–	–/–	–	–	–/–
4j		3.0	8.1	38	1.6/1.3	9.9	2.1	1.4/0.2
4k		8.6	18	17	1.4/1.0	0.8	12	1.7/0.9
4l		3.8	6.0	11	1.1/0.8	>10	1.3	0.4/0.1
4m		15	49	–	2.1/1.1	>10	–	0.4/0.4

Table 3
SAR at middle ring and $R^3/R^4/R^5$

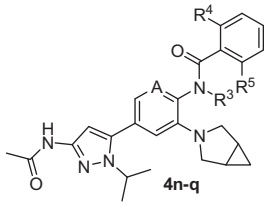

Compd ID	A/R^3	R^4/R^5	RORγ Fret IC_{50} (nM)	RORγ Gal4 EC_{50} (nM)	Splenocyte IL17 EC_{50} (nM)	RORα/RORβ EC_{50} (μM)	PXR act. EC_{50} (μM)	Solubility (μg/mL)	PPB fu% Human/rat
4n	CH/CH_3	F/Cl	4.9	10	110	1.9/1.7	–	–	0.9/0.2
4o	CH/CD_3	Cl/Cl	3.4	6.1	73	1.5/0.6	0.5	0.8	0.4/0.1
4p	CH/CD_3	F/Me	4.8	12	355	2.0/1.5	>10	17	1.1/0.2
4q	N/CD_3	F/Cl	9.2	33	–	>10/6.2	1.3	48	5.6/2.2

(ortho- to the aniline nitrogen) yielded **4q** with excellent kinetic solubility (48 μg/mL) and free levels against plasma proteins albeit with slight decrease in cellular potency.

Since the methyl group of acetamide head group is predicted to point to the open region based on docking studies (Data not shown), it is reasoned that introduction of additional groups at this position (R^6) might retain potencies. In Table 4, a series of amides (**4r–y**), ureas (**4z**, **5a–d**) and carbamates (**5e–f**) were synthesized. These analogues showed comparable potencies to **4j** in the RORγ GAL4 assay but were in general less potent in the splenocyte assay with the exception of **4s**.

Based on docking studies, substitutions off pyrazole ring at the R^7 position occupy the same space as chlorine atom on **4a** does. However, due to the ring difference (pyrazole vs phenyl) a methyl group (similar in size to Cl) off pyrazole scaffold does not provide comparable potency (data not shown). A number of analogues were made and their profiles were shown in Table 5. Cyclopentyl analogue **5g** is equally potent to **4j** but with inferior physical properties that may be due to the higher lipophilicity of a cyclopentyl group as to an isopropyl group. Both cyclobutyl and cyclopropylmethylene analogues **5h** and **5k** had 5-fold decreases in potencies in the splenocyte vs. **4j**. The isopropyl group at this position (R^7) offers a balance between potency and physical properties.

A combination of pyridine central ring with a piperidine substitution at R^2 gave **5m** with reasonable profile (Table 6). It has 34 nM in the mouse splenocyte assay, selective over RORα/RORβ and PXR receptor, and has good kinetic aqueous solubility (37.4 μg/mL) and free unbound levels in plasma proteins (Human: 7.6%; Rat: 1.3%). Compound **5m** has an oral exposure of 927 ng h/mL when dosed in rats at 10 mpk (0–7 h, CMC/Tween) and 2259 ng h/mL when dosed in mouse at 25 mpk (CMC/Tween). A thiazole analogue **5n** with the same substitution (isopropyl and acetamide) is equally potent but has poor physical property as well as PXR activation. Neither triazole (**5o**) nor imidazole (**5p**) showed activity in the concentration range tested.

A representative synthesis is shown in Scheme 1. Nucleophilic aromatic substitution of **6** with amine **7** gave **8**. Reduction of **8** followed by amide formation yielded **10**, which was then methylated and converted to the corresponding boronic ester **11**. The other key intermediate **12** was prepared in 6 steps. Regioselective alkylation of 3-nitropyrazole **13** gave **15**. Iron powder reduction of **15** followed by protection of the newly installed amino group yielded intermediate **17**. Bromination of **17** followed by deprotection and acetylation produced aminopyrazole **12**. Cross coupling of **11** with **12** furnished the target **4j**.

Table 4
SAR at R^6 position

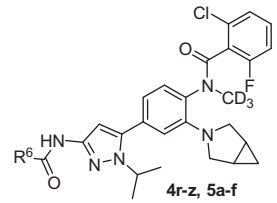

Compd ID	R^6	RORγ Fret IC_{50} (nM)	RORγ Gal4 EC_{50} (nM)	Splenocyte IL17 EC_{50} (nM)
4r	H	4.9	22	–
4s	Et	4.9	14	33
4t	Cyclopropyl	5.0	7.6	88
4u	^iPr	–	15	128
4v		–	15	134
4w		12	12	134
4x	$HOCH_2$–	3.3	15	120
4y		70	93	–
4z		6.0	25	354
5a		16	22	148
5b		9.4	21	–
5c	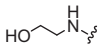	18	37	–
5d		–	71	–
5e		21	57	–
5f		–	150	–

An X-ray structure of human RORγ ligand binding domain in complex with **4j** to 2.2 Å was generated (PDB Code: 4ZOM, Fig. 2A). The structure shows the carbonyl group on the pyrazole head group makes a hydrogen bond interaction with the backbone NH of Glu379 at the entrance of the ligand binding site (Fig. 2B). The middle phenyl ring is sandwiched between Phe358 and Met365, while the azabicyclo[3.1.0]hexane substituent travels into sub-pocket making hydrophobic interactions with the side chains of Phe388, Ile397, Ile400 and Phe401 (Fig. 2C). The Cl/F benzamide

Table 5
SAR at R^7 position

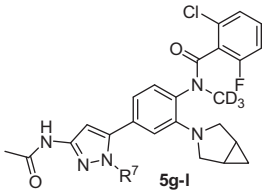

Compd ID	R^7	RORγ Fret IC_{50} (nM)	RORγ Gal4 EC_{50} (nM)	Splenocyte IL17 EC_{50} (nM)	RORα/RORβ EC_{50} (μM)	PXR act. EC_{50} (μM)	Solubility (μg/mL)	PPB fu% Human/rat
5g		5.1	9.5	60	1.3/1.3	0.5	0.1	0.2/<0.05
5h		5.2	13	199	–/–	–	0.5	0.3/0.04
5i		15	55	–	–/–	–	0.8	–/–
5j		40	76	–	–/–	–	–	–/–
5k		6.4	12	201	1.8/1.8	8.8	10.1	0.5/0.2
5l		8.4	17	–	9.3/1.3	0.9	0.5	–/–

Table 6
Other 5-membered heteroaryls

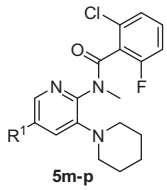

Compd ID	R^1	RORγ Fret IC_{50} (nM)	RORγ Gal4 EC_{50} (nM)	Splenocyte IL17 EC_{50} (nM)	RORα/RORβ EC_{50} (μM)	PXR act. EC_{50} (μM)	Solubility (μg/mL)	PPB fu% Human/rat
5m	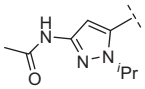	6.2	13	34	9.3/2.3	5.4	37.4	7.6/1.3
5n	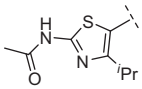	3.2	10	–	2.2/0.8	0.4	0.3	0.3/0.2
5o	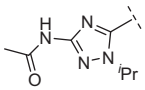	>5000	>1000	–	–/–	–	–	–/–
5p	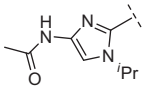	4800	>1000	–	–/–	–	–	–/–

tail piece travels towards the junction of helix 3, 6, 7 and 11 of RORγ and is buried in a pocket composed of Trp317, Leu483, Phe486, Leu396, Cys393, Ile397 and Leu392. The carbonyl of the linker amide makes a hydrogen bond with the imidazole NH of His479 (Fig. 2D).

By superimposing the RORγ **4j** structure with the 25-hydrocholesterol agonist co-crystal structure (PBD code: 3L0L),[21] a hypothesis can be generated for how **4j** achieves inverse agonism. RORγ has a signature hydrogen bond between His479 of helix 11 and Tyr502 of helix 12 which locks RORs in the agonist conformation creating part of the co-activator binding pocket.[19] In the **4j** co-crystal structure His479 is seen in an alternate conformation from the 25-hydroxycholesterol agonist structure where it now makes a hydrogen bond with the carbonyl of the benzamide (Fig. 3A). Additionally, Trp317 of helix 3 is seen in an alternate conformation where the head piece of the benzamide pushes tryptophan side chain out towards helix 12 where it clashes with Tyr502 (Fig. 3B). Both interactions disrupt the His479 and Tyr502 hydrogen bond unlocking the agonist conformation and might explain how **4j** achieves inverse agonism.

In summary we have identified a series of novel pyrazole containing benzamides as potent RORγ inverse agonists. We have

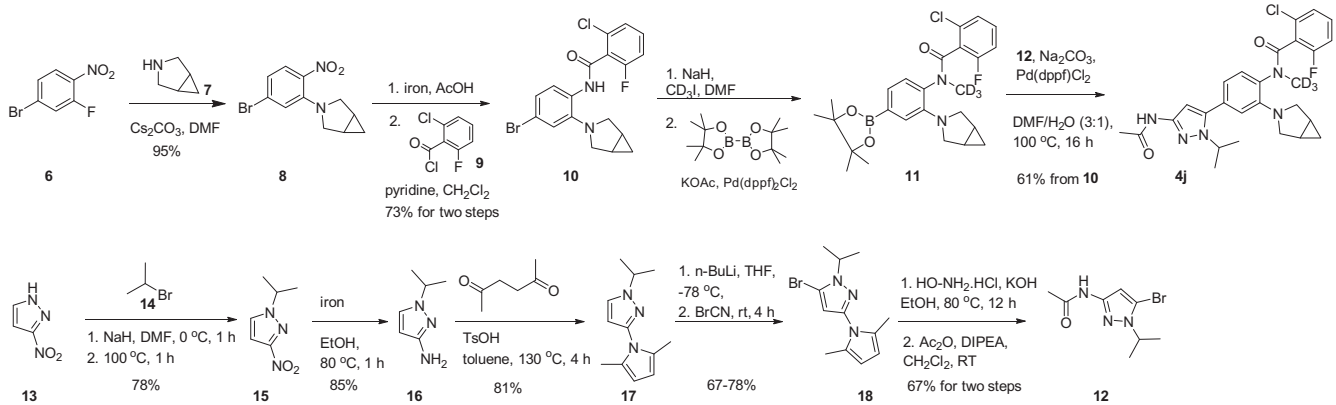

Scheme 1.

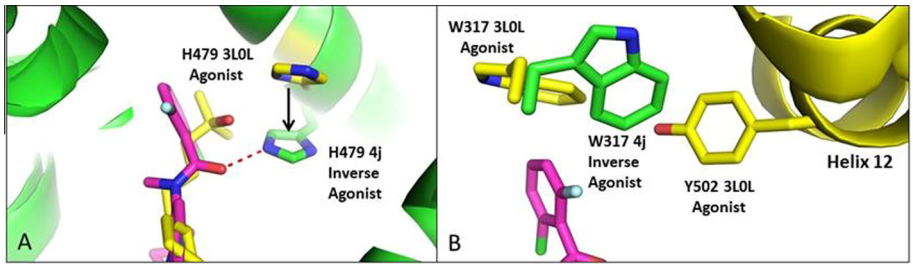

Figure 3. Superposition of RORγ/**4j** Cocrystal structure (Green/Magenta) with the 25-hydroxycholesterol structure (3L0L, Yellow). (A) His479 shifts away from agonist conformation to hydrogen bond with carbonyl of **4j**. (B) Tail benzamide of **4j** moves Trp317 towards Helix 12 clashing with Tyr502.

improved the cellular potency as well as physical properties. Compounds such as **4j** and **5m** are potent and selective and have adequate profiles that would allow them to be used as probe compounds for further study of the RORγ biology.

Acknowledgments

We thank Harriet Rivera for compound management support and Meimei Wen, Ph.D. for NMR structure determination support.

References and notes

1. Fauber, B. P.; Magnuson, S. *J. Med. Chem.* **2014**, *57*, 5871.
2. Huh, J. R.; Littman, D. R. *Eur. J. Immunol.* **2012**, *42*, 2232.
3. Jetten, A. M. *Nucl. Recept Signal.* **2009**, *7*, e003.
4. Ghoreschi, K.; Laurence, A.; Yang, X. P.; Hirahara, K.; O'Shea, J. J. *Trends Immunol.* **2011**, *32*, 395.
5. Sutton, C. E.; Mielke, L. A.; Mills, K. H. *Eur. J. Immunol.* **2012**, *42*, 2221.
6. Langley, R. G.; Elewski, B. E.; Lebwohl, M.; Reich, K.; Griffiths, C. E. M.; Papp, K.; Puig, L.; Nakagawa, H.; Spelman, L.; Sigurgeirsson, B.; Rivas, E.; Tsai, T.-F.; Wasel, N.; Tyring, S.; Salko, T.; Hampele, I.; Notter, M.; Karpov, A.; Helou, S.; Papavassilis, C.; ERASURE Study Group; FIXTURE Study Group *N. Engl. J. Med.* **2014**, *371*, 326.
7. Mease, P. J. *Curr. Opin. Rheumatol.* **2015**, *27*, 127.
8. Huh, J. R.; Leung, M. W.; Huang, P.; Ryan, D. A.; Krout, M. R.; Malapaka, R. R.; Chow, J.; Manel, N.; Ciofani, M.; Kim, S. V.; Cuesta, A.; Santori, F. R.; Lafaille, J. J.; Xu, H. E.; Gin, D. Y.; Rastinejad, F.; Littman, D. R. *Nature* **2011**, *472*, 486.
9. Solt, L. A.; Kumar, N.; Nuhant, P.; Wang, Y.; Lauer, J. L.; Liu, J.; Istrate, M. A.; Kamenecka, T. M.; Roush, W. R.; Vidović, D.; Schürer, S. C.; Xu, J.; Wagoner, G.; Drew, P. D.; Griffin, P. R.; Burris, T. P. *Nature* **2011**, *472*, 491.
10. Ivanov, I. I.; McKenzie, B. S.; Zhou, L.; Tadokoro, C. E.; Lepelley, A.; Lafaille, J. J.; Cua, D. J.; Littman, D. R. *Cell* **2006**, *126*, 1121.
11. Isono, F.; Jujita-Sato, S.; Ito, S. *Drug Discovery Today* **2014**, *19*, 1205.
12. René, O.; Fauber, B. P.; Boenig, G. d. L.; Burton, B.; Eidenschenk, C.; Everett, C.; Gobbi, A.; Hymowitz, S. G.; Johnson, A. R.; Kiefer, J. R.; Liimatta, M.; Lockey, P.; Ouyang, W.; Wallwebe, H. A.; Wong, H. *ACS Med. Chem. Lett.* **2015**, *6*, 276.
13. Fauber, B. P.; Rene, O.; Burton, B.; Everett, C.; Gobbi, A.; Hawkins, J.; Johnson, A. R.; Liimatta, M.; Lockey, P.; Norman, M.; Wong, H. *Bioorg. Med. Chem. Lett.* **2014**, *24*, 2182.
14. Van Niel, M. B.; Fauber, B. P.; Cartwright, M.; Gaines, S.; Killen, J. C.; René, O.; Ward, S. I.; Boenig, G. L.; Deng, Y.; Eidenschenk, C.; Everett, C.; Gancia, E.; Ganguli, A.; Gobbi, A.; Hawkins, J.; Johnson, A. R.; Kiefer, J. R.; La, H.; Lockey, P.; Norman, M.; Ouyang, W.; Qin, A.; Wakes, N.; Waszkowycz, B.; Wong, H. *Bioorg. Med. Chem. Lett.* **2014**, *24*, 5769.
15. Xiao, S.; Yosef, N.; Yang, J.; Wang, Y.; Zhou, L.; Zhu, C.; Wu, C.; Baloglu, E.; Schmidt, D.; Ramesh, R.; Lobera, M.; Sundrud, M. S.; Tsai, P.-Y.; Xiang, Z.; Wang, J.; Xu, Y.; Lin, X.; Kretschmer, K.; Rahl, P. B.; Young, R. A.; Zhong, Z.; Hafler, D. A.; Regev, A.; Ghosh, S.; Marson, A.; Kuchroo, V. K. *Immunity* **2014**, *40*, 477.
16. Wang, Y.; Cai, W.; Zhang, G.; Yang, T.; Liu, Q.; Cheng, Y.; Zhou, L.; Ma, Y.; Cheng, Z.; Lu, S.; Zhao, Y.-G.; Zhang, W.; Xiang, Z.; Wang, S.; Yang, L.; Wu, Q.; Orband-Miller, L. A.; Xu, Y.; Zhang, J.; Gao, R.; Huxdorf, M.; Xiang, J.-N.; Zhong, Z.; Elliott, J. D.; Leung, S.; Lin, X. *Bioorg. Med. Chem.* **2014**, *22*, 692.
17. Example 136 in WO2014/008214.
18. Assay condition in WO2014/008214. Ligand binding domain of RORγ was used.
19. Assay condition in WO2014/008214.
20. Gant, T. G. *J. Med. Chem.* **2014**, *57*, 3595.
21. Jin, L.; Martynowski, D.; Zheng, S.; Wada, T.; Xie, W.; Li, Y. *Mol. Endocrinol.* **2010**, *24*, 923.